Biosensors and Bioelectronics 26 (2011) 2334–2340

Contents lists available at ScienceDirect

Biosensors and Bioelectronics

journal homepage: www.elsevier.com/locate/bios

TiO_2 nanowire FET device: Encapsulation of biomolecules by electro polymerized pyrrole propylic acid

Yung-Ming Chu [a], Chi-Chang Lin [b], Hsien-Chang Chang [a,*], Changming Li [c], Chunxian Guo [c]

[a] Institute of Biomedical Engineering, National Cheng Kung University, No. 1, University Road, Tainan 70101, Taiwan
[b] Department of Chemical and Materials Engineering, Tunghai University, Taichung 40704, Taiwan
[c] Division of BioEngineering, School of Chemical and Biomedical Engineering, Nanyang Technological University, Singapore 637457, Singapore

ARTICLE INFO

Article history:
Received 2 September 2010
Accepted 6 October 2010
Available online 14 October 2010

Keywords:
TiO_2 nanowire
Pyrrole propylic acid
Electropolymerization
Field effect transistor
Biosensor

ABSTRACT

Silane-based methods have become the standards for the conjugation of biomolecules, especially for the preparation of one-dimensional nanomaterial biosensors. However, the specific binding of those target molecules might raise problems with regard to the sensing and non-sensing regions, which may contaminate the sensing devices and decrease their sensitivity. This paper attempts to explore the encapsulation of biomolecules on a one-dimensional nanomaterial field effect transistor (FET) biosensor using polypyrrole propylic acid (PPa). Specifically, the encapsulation of biomolecules via the electropolymerization of pyrrole propylic acid (Pa), a self-made low-conductivity polymer, on TiO_2-nanowire (NW)-based FETs is presented. The energy dispersive spectrum (EDS) was obtained and electrical analysis was conducted to investigate PPa entrapping anti-rabbit IgG (PPa/1°Ab) on a composite film. The specificity, selectivity and sensitivity of the sensor were analyzed in order to determine the immunoreaction of PPa/1°Ab immobilized NW biosensors. Our results show that PPa/1°Ab achieved high specificity immobilization on NWs under the EDS analysis. Furthermore, the TiO_2-NW FET immunosensor developed in this work successfully achieved specificity, selectivity and sensitivity detection for the target protein rabbit IgG at the nano-gram level. The combination of PPa material and the electropolymerization method may provide an alternative method to immobilize biomolecules on a specific surface, such as NWs.

1. Introduction

In recent years, one-dimensional (1-D) nanomaterials (e.g., nanowires, nanorods and nanotubes) field effect transistors (FETs) have attracted much attention in biosensing research and related applications due to their high sensitivity and specificity for rapid analyte detection (Cui et al., 2001a; Patolsky et al., 2006a; He et al., 2008). Many studies have illustrated the fabrication of nanostructure sensors using semiconducting 1-D titanium dioxide (TiO_2) materials. Immunosensors and gas sensors made of TiO_2 nanowire (NW) devices have been successfully developed with acceptable sensitivity for *Listeria monocytogenes*, humidity and hydrogen gas detection (Varghese et al., 2003; Li et al., 2010; Wang et al., 2008). A TiO_2 matrix with a 1-D structure is an easily manufactured material with stable chemical and photo-chemical properties, as well as biocompatibility in biological systems (Li et al., 2010; Bao et al., 2008). An important benefit of 1-D nanostructure TiO_2 materials is their wide energy band gap (between 1.8 and 4.1 eV), which may provide a better sensitivity range than those of other available matrices for FETs (Wang et al., 2008).

The specific antibody–antigen reaction is an important part of all nanostructure-based materials for biosensors and immunosensors. Here, biomolecules provide the specific ability to recognize target substances (e.g., proteins, antigens, and peptides) via affinity adsorptions. Many chemical- and physical-based methods, such as silane linking (e.g., APTMS, APTES or APDMES) or polymer entrapment (e.g., PEI/PEG), are well-established protocols for immobilizing biomolecules on matrices (Star et al., 2003; Katz and Willner, 2004; Zheng et al., 2005; Byon et al., 2008). To date, the majority of research on biomolecule immobilization methods has been on the sensing and non-sensing regions. A number of studies have shown that biomolecules can be encapsulated via the electrochemical polymerization (ECP) of a conducting polymer on the sensing area of the biosensor device (Lange et al., 2008; Ramanathan et al., 2007). Unfortunately, the thin-film formation via the polymerization of conducting polymers used in ECP – based immunosensor studies seems to be inapplicable to 1-D nanomaterials for FET biosensor development, as an FET sensor coated with a higher conductivity ECP may lose its semiconductor functions owing to increasing the electron transfer rate. In our previous works, a self-made electrochemical polymerizable con-

* Corresponding author. Tel.: +886 6 2757575x63426; fax: +886 6 2343270.
E-mail addresses: hcchang@ccmail.ncku.edu.tw, hcchang@mail.ncku.edu.tw (H.-C. Chang).

0956-5663/$ – see front matter
doi:10.1016/j.bios.2010.10.006

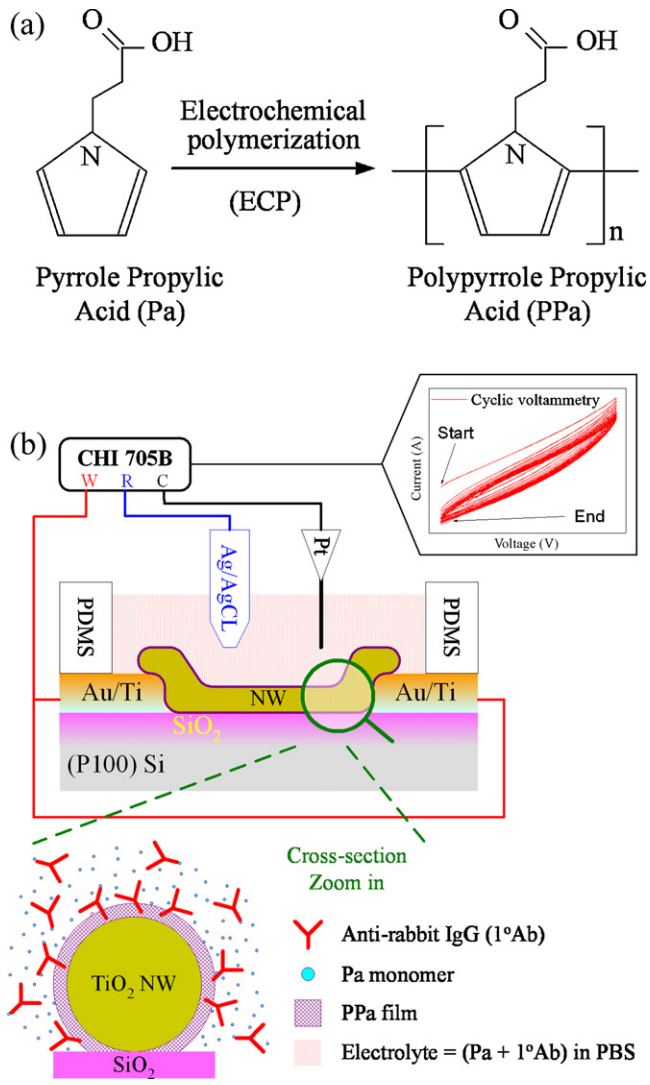

Fig. 1. (a) Structure of pyrrole propylic acid before and after ECP, and (b) the experiment setup of the ECP system.

ducting material, polypyrrole propylic acid (PPa), was shown to be a good material for immunosensor development because of its poorer conductivity compared to those of other commonly used materials (e.g., polyaniline, polypyrrole) (Lange et al., 2008; Gerard et al., 2002) (Fig. 1a). More details on the preparation and characterization of PPa can be founded in our previous works (Dong et al., 2006, 2007; Hu et al., 2007), and the practicality of the proposed PPa material and biomolecule immobilization approach were demonstrated through the TiO_2-NW-based FET.

This study focuses on an elementary understanding of biomolecule encapsulation on a 1-D nanomaterial FETs biosensor by PPa, and the basic operating protocol for the ECP of PPa/biomolecules matrices is also provided. Immunoglobulin G is a commonly used protein for the specific adsorption of biomolecules, and has been well studied in much previous research on immunosensors and immunoanalyzation (Dong et al., 2006; Storri et al., 1998; Wilson and Nie, 2006; Chen et al., 2010; Hu et al., 2010). In this paper, the anti-rabbit IgG was selected as the receptor protein (1°Ab), which was encapsulated on the TiO_2-NW-FET-based electronic immunosensor via polymerization of a low-conductivity polymer for specific recognition of an antigen (rabbit IgG, 2°Ab). In brief, specific 1°Ab was encapsulated via the ECP of PPa film onto the patterned TiO_2 NW surface for affinity reaction. The conductance changes during the modification processes were measured and recorded. The before and after affinity binding were analyzed. The fabrication processes, detection mechanisms, and advantages of using PPa are described in detail.

2. Experimental details

2.1. TiO_2-NW-based FET device

The fabrication of the NW-based FET device was similar to as stated in previous works, with some slight modifications. The first step was the synthesis of TiO_2 NWs by using a simple hydrothermal method. Briefly, 75 mg of TiO_2 powder (Degussa P25) was added to 10 mL of 10 M NaOH solution in a Teflon-lined autoclave and placed in a furnace at 200 °C for 24 h, and then cooled to room temperature (RT). The resulting product, sodium titanate ($Na_2Ti_3O_7$) NWs, was then transformed into hydrogen titanate ($H_2Ti_3O_7$) NWs after being immersed in 50 mL of 1 M HNO_3 for 1 h and washed with 3 L of deionized water. TBAOH (tetrabutylammonium hydroxide) solution containing 1 mg/mL of $H_2Ti_3O_7$ NWs was then pulled and spin-coated onto the silicon substrate (P100, resisitivity: 0.01–0.05 Ω, 100-nm-thick thermal oxide layer at polished side) with patterned 15 μm gap gold/titanium (150/50 nm) electrodes. An average of 72 ± 10 pieces of the NW-coated substrate with an area of 100 μm^2 was obtained from each batch procedure. The coated $H_2Ti_3O_7$ NWs devices were then further transformed into TiO_2 NWs devices after 3 h of thermal treatment at 650 °C.

2.2. Encapsulization of biomolecules on the device

The three-electrode system setup for encapsulating structured PPa/1°Ab on the TiO_2-NW FET device via ECP is illustrated in Fig. 1b. Based on the method in previous research and with slight modifications, the following conditions were used for the parameters and electrolyte concentration throughout this work (Dong et al., 2006, 2007, 2008; Hu et al., 2007, 2008; Lu and Li, 2008.). The electrolyte was prepared by adding 100 μg/mL of 1°Ab to phosphate buffered saline (10 mM PBS) containing 15 mM of pyrrole propylic acid (Pa) monomer under gentle mixing at 25 °C for 15 min. The mixed solution was cast and a thin PPa/1°Ab film formed on the surface of the TiO_2 NW after ECP using the cyclic voltammetry method (voltage of 0 to 0.76 V for 20 cycles, scan rate of 0.1 V/s, Ag/AgCl reference electrode and Pt counter electrode). The current–voltage diagram shows that the current increased dramatically in the first 20 cycles, which indicates that the mixture of PPa/1°Ab was gradually polymerized on the surfaces of TiO_2 NWs and the metal. After 20 scanning cycles, the observed saturation current indicated that the formation of a PPa/1°Ab film. Biomolecules can be attached to the PPa surface or entrapped in the PPa polymer network easily owing to its enriched carboxyl groups (Dong et al., 2006). To develop 1-D based immunosensors, the biomolecule copolymer film was further embedded specifically on the surface of the NW, which may preventing contamination of biomolecules on non-target areas (out of NWs).

2.3. Analyte properties

All analyte solutions containing 2°Ab and anti-human IgA were prepared from stock solutions by a series of dilutions in 10 mM PBS. Adjusted 2°Ab with final concentrations of 119 pg/mL, 1.19 ng/mL, 2.38 ng/mL, 5.95 ng/mL, and 11.9 ng/mL were obtained for the performance studies, including specificity, selectivity and sensitivity analyses. Another adjusted mixture with 12.3 ng/mL of anti-human IgA was used for the selectivity analysis. Briefly, the prepared PPa/1°Ab-coated device was exposed to 10 μL of the above-mentioned analyte solutions at RT for 5 min. The device was

then thoroughly rinsed three times with 10 mM PBS and deionized water, then subsequently dried under N_2 gas and placed in a vacuum oven at RT for 5 min. After drying, the biomolecule conjugated PPa/1°Ab-coated device was assembled and connected to the electrical analyzer for electrical properties analysis.

2.4. Morphology and structure of the NWs

A scanning electron microscope (SEM, JEOL 6700F) and transmission electron microscope (TEM, Hitachi H-7500) were used to analyze the morphology of the NW and devices. The surfaces of the NWs were coated with ultra-thin gold layer and examined under an SEM operated at a 10 kV accelerating voltage. An energy dispersive X-ray spectroscope (EDS, OXFORD INCA400) was attached to the SEM. Moreover, Raman scattering spectrum analysis (Raman, Thermo DXR) was conducted to further characterize the prepared NWs specimens.

2.5. X-ray microanalysis of the devices

To obtain the PPa/1°Ab distributions and locations on the NW-devices, element analyses were conducted using EDS. The devices were examined under an SEM operated at a 15 mm working distance and 13 A probe current. The spectrum acquisition setup of the element distribution was collected using the line-mapping mode and an X-ray detector operated at one process time and 600 s acquisition time. The spectrum acquisition setup of the element ratio was collected using the rectangle-scanning mode and an X-ray detector operated at six process times and 100 s live-time.

2.6. Electrical measurements

A characterization curve plot showing the changes in the drain current (I_D) together with drain-source voltages (V_{DS}) is an important diagram to better understand the electrical properties of such devices. Briefly, the analyzing probes, which act as the back-gate, drain, and source electrodes, were connected between the analyzed device and Sourcemeter system (KEITHLEY, 2612) via the triaxial cables, and the signal was recorded using LabTracer. Various gate-source voltages (V_{GS}) were applied to the silicon substrate (V_{GS} = −4 to 8 V) to monitor the changes of I_D for −5 to 10 V of sweep V_{DS}. To avoid external electrical interference on the measurement results at the lower current analysis, all of the electrical analysis in this work was prepared and undertaken within a shielding box.

3. Results and discussions

The major focus of this research was to develop an alternative method to the conventional silane linker approach for biomolecule immobilization, which may easily contaminate non-sensing regions and cause lower sensitivity. To accomplish this, the ECP method was applied and investigated for in situ polymerization of PPa/1°Ab on a 1-D nanomaterial FET. The investigation centered on PPa immobilization and TiO_2 NW-based FETs, as a number of factors indicate that these matrices may be suitable for the particular demands of an immunosensor. The preparation and characterization procedure of the TiO_2-NW and TiO_2-NW-based FET device, and the ECP of PPa together with IgG molecules will be fully studied in this work, along with the specific recognition of target proteins. The sensitivity of the designed TiO_2-NW FET is also presented.

3.1. Characteristics of TiO_2 NWs and TiO_2-NW-based FET device

The morphologies and structural properties of TiO_2 NWs and the related FET device were characterized under SEM and TEM. Fig. 2a and b shows the SEM and TEM images of TiO_2 NWs, respectively. The average diameter and length of the prepared NWs were 40–50 nm and 10–20 μm, respectively. As can be seen, no core-shell structure was observed in the fabricated NWs. Fig. 2c shows the Raman scattering spectrum of the NWs under 532-nm laser excitation. Three characteristic peaks at 396, 515, and 638 cm^{-1} indicate the prepared TiO_2 NWs have the anatase structure. These

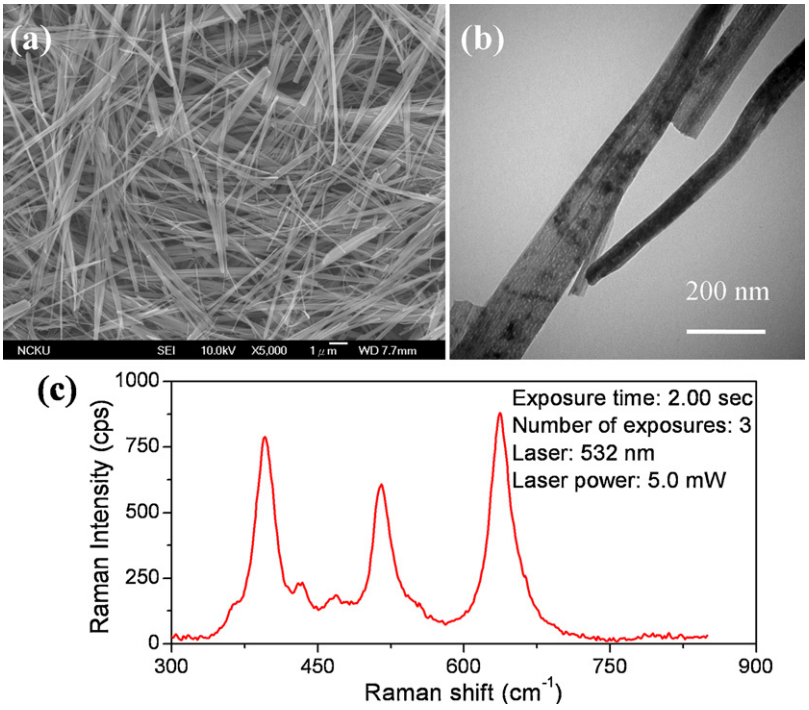

Fig. 2. (a) SEM image showing the diameter and length of TiO_2 NWs, which were calculated to be 40–50 nm and 10–20 μm, respectively. (b) TEM image showing the NW structure of the prepared TiO_2 matrix in which no material core-shell was observed. (c) Raman spectrum of TiO_2 NWs measured using a laser at a 532 nm wavelength. The characteristic peaks at 396, 515, and 638 cm^{-1} indicate that the prepared TiO_2 NWs has an anatase structure.

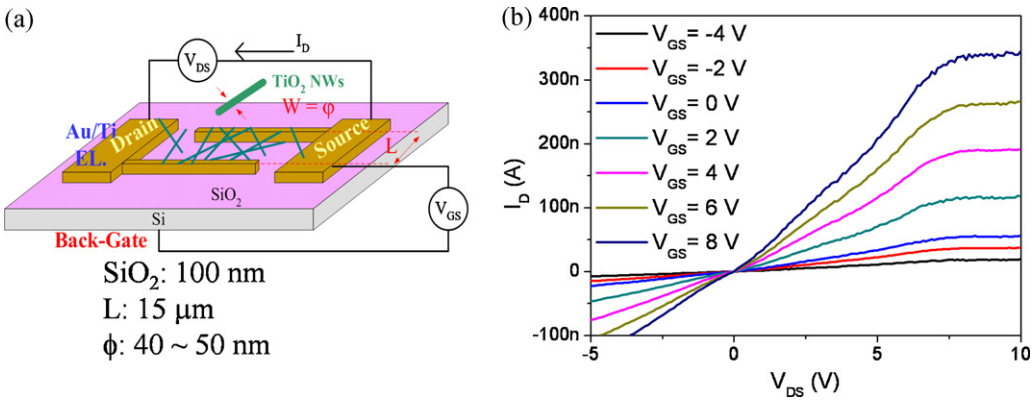

Fig. 3. (a) Schematic diagram of bottom-gated multiwire TiO_2 NW device. (b) Gate-source voltage of TiO_2 NWs was measured to determine the relationship between the channel drain current and the drain-source voltage under various applied gate-source voltages. The complementary behavior indicated that the I_D–V_{DS} responses of prepared TiO_2 NWs were similar to those of n-type semiconductors.

results are also in agreement with those presented by Papp et al. (2005). These analyses again indicate that the simple hydrothermal method can be used in order to synthesize TiO_2 NWs with an anatase structure.

Further analyses were conducted to understand the electrical characteristics of the prepared TiO_2-NW FET device. Fig. 3a shows a schematic diagram of a bottom-gated multiwire TiO_2-NW-based FET device and the experimental setup for the electrical measuring system. The gate voltage of TiO_2 NWs was measured to obtain the relationship between the channel drain current and the drain-source voltage under various applied gate-source voltages. As shown in Fig. 3b, an increased I_D tendency can be observed at a larger positive V_{GS} in the prepared TiO_2 NWs device, which indicated that our designed device acts similar to an n-type FET, and this result is consistent with those reported for other n-type 1-D nanomaterial FET studies (Jin et al., 2004; Patolsky et al., 2006b).

3.2. ECP encapsulation of biomolecules

The surface of the TiO_2-NW FET device was examined using EDS analysis to confirm the ECP of PPa and the encapsulation 1°Ab. Fig. 4a and b shows the EDS analysis results, which were used to identify the polymerization or the contamination locations of prepared PPa/1°Ab-coated TiO_2-NW FETs and untreated TiO_2-NW FETs in both the target (NWs) and non-target areas (NWs free) of the titanium/carbon element spectra. The line-mapping results in Fig. 4a show that two significant signals from contributed titanium (blue curve) are expressed on the NWs. After the polymerization of PPa/1°Ab on the surface of TiO_2 NWs, signals from carbon (red curve) exhibited a similar pattern, with two significant peaks at the same places as those of titanium. This demonstrates that most of the biomolecules and PPa were electrically polymerized only on the NWs surface. Here the TiO_2-NW-only group, without PPa/1°Ab coating, is also presented for comparison with the effect of the ECP processes (Fig. 4b). Before ECP, the line-mapping analysis shows only one strong peak from titanium can be observed. In addition, the weight percentages and distributions of the major elements (i.e. C, O, Ti and Au) before and after ECP of PPa/1°Ab on the surface of NWs and substrates are summarized in Fig. 4c. As can be seen, the weight percentages of oxygen and silicon were the dominant ones on the Si/SiO_2 substrate, and the percentage of other elements on the NWs surface did not significantly change, even after the ECP of PPa/1°Ab. Moreover, before/after the surface modification, no carbon elements were found on the NW-free area, which indicates

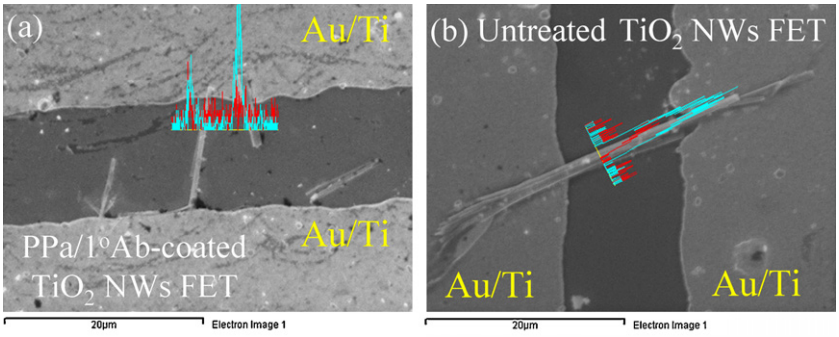

(c)

Weight%	Microelectrode (area)				Substrate (area)		
Element	C	O	Ti	Au	C	O	Si
Untreared TiO2 NWs FET	--	7.73	4.01	88.25	--	52.10	47.90
TiO2 NWs FET (electropolymerization)	2.19	6.89	3.24	87.67	--	53.54	46.46

Fig. 4. The EDS analyses show the distribution and percentage of elements in the TiO_2-NWs FET devices with and without PPa/1°Ab coating. The line-mapping results represent the devices (a) with and (b) without PPa/1°Ab coating, and the blue and red spectra show the distributions of titanium and carbon, respectively. A significantly higher carbon spectrum can be found for the PPa/1°Ab-coated device when compared to that for the device without this coating. (c) EDS rectangle-scanning results for TiO_2-NWs FET devices. The substrate-only area was measured as the background for comparison with the Pa/1°Ab modified microelectrode area. (For interpretation of the references to color in this figure legend, the reader is referred to the web version of the article.)

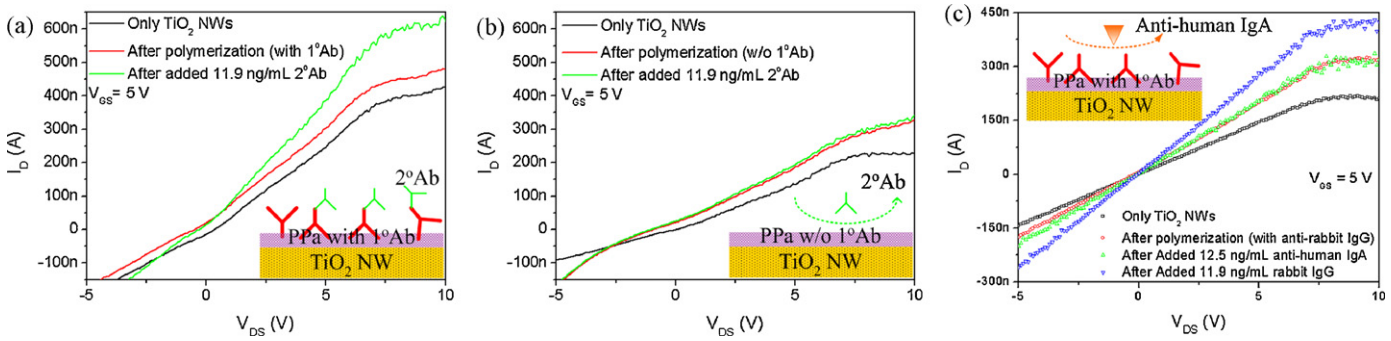

Fig. 5. I_D–V_{DS} curve showing the specificity and selectivity of the TiO_2-NW-based immunosensor (a) with and (b) without immobilization of 1°Ab for 2°Ab detection. A change of about 75 nA in the drain current was observed in the 1°Ab-immobilized group after addition of 2°Ab under the applied conditions of V_{DS} = 5 V and V_{GS} = 5 V (a). In contrast, a negligible current change was found for the PPa-coated group device (without 1°Ab) (b). A similar pattern with negligible current change was observed after addition of anti-human IgA on the PPa/1°Ab-coated device. In contrast, a significant change can be observed on same device after addition of 2°Ab (c).

the PPa was electrochemically polymerized only on the NWs surface. These unchanged elements (Si, O and C) indicate that the ECP processes can be controlled at a specific area (e.g., NWs surface in this case) without any unexpected adsorption or contamination. The weight percentages of the four major elements on the Au/Ti electrode were also analyzed. As the gold element comes from the patterned gold electrode, the titanium may come from the TiO_2 NWs, and the oxygen was contributed from both the substrate and the NWs. Similar weight percentage ratios can be found for the three elements in both the untreated and study groups. In contrast, only the carbon ratio increased significantly, from an undetectable level to about 2.2%, which suggests PPa/1°Ab was successfully electrical polymerized on the NWs surface of the treated group.

As data shown in Fig. 4, the carbon element, which is dominated by Pa and 1°Ab on the TiO_2-NW devices, can be analyzed via the change in chemical composition before and after ECP. Electrochemical polymerized Pa may have great ability for encapsulating biomolecules, especially on the sub-micron scale (i.e., nanomaterials) without contaminating non-target areas, and this might be expected to increase the sensitivity of the device. In addition, one of the aims of this study was to explore the feasibility of biomolecule encapsulation on a 1-D nanomaterial FETs biosensor using PPa. In order to ensure the immobilized 1°Ab was saturated on the TiO_2 NWs, which provides a greater sensing ability due to a high proteins/NWs ratio, an electrolyte a high concentration of 1°Ab was applied for the ECP reaction (Cui et al., 2001b). It is worth noting that the number of immobilized proteins on NW can be further controlled and adjusted via a well controlled scan rate and the number of scan cycles in cyclic voltammetry, as discussed in previous studies (Cosnier et al., 1999; Kwon et al., 2006; Kum et al., 2007).

3.3. Specificity and selectivity analysis

To confirm the specific recognition capability of the PPa/1°Ab-coated TiO_2-NW FET device, the signal for electrical response before and after reaction with 2°Ab was studied and analyzed. Fig. 5a and b shows the I_D–V_{DS} curves to illustrate the difference in electrical characteristics after immunoreaction with 11.9 ng/mL of 2°Ab on both PPa/1°Ab and PPa modified TiO_2-NW-FET devices, respectively. Fig. 5a shows significant changes in the response of I_D with the addition of 2°Ab to the PPa/1°Ab-coated device. Significant increases in I_D were observed before and after ECP of PPa/1°Ab compared to the PPa-only group (Fig. 5b). Although PPa is a poor conductive polymer (about 52.1 μS/cm in this study), it still provides a few conducting path for carriers, which may lead to a slight increase in I_D (increased conductance) (Dong et al., 2006). The anti-rabbit IgG (1°Ab) was encapsulated on the TiO_2 NW surface to specifically capture target rabbit IgG (2°Ab), and the PPa-coated TiO_2-NWs FET served as the control group (electrolyte without 1°Ab or any other protein). The captured 2°Ab induced carrier capture along the PPa/1°Ab-coated TiO_2 NWs, leading to an increase in I_D. The negligible I_D change during the immobilization of IgG and the increased I_D caused by the target protein (2°Ab) are in agreement with some previous studies (Curreli et al., 2008).

To confirm the selectivity of the developed biosensors, solutions of anti-human IgA and rabbit IgG (as 2°Ab in this work) were added in sequence onto the same TiO_2-NW biosensor, as described in the methodology section. Fig. 5c shows the I_D value of the I_D–V_{DS} curve after 10 μL of analyte solutions were dropped on the PPa/1°Ab-coated TiO_2 NW device. As can be seen clearly, the I_D–V_{DS} curve has a similar pattern before and after the introduction of 12.3 ng/mL of anti-human IgA, in contrast, an increasing tendency can be observed when the 11.9 ng/mL of 2°Ab was applied. A significant selectivity binding can thus be found during the stepwise reaction of the NW device to anti-human IgA and 2°Ab (rabbit IgG). These clear results again demonstrate that our FET-based biosensor has acceptable selectivity and specificity with regard to affinity adsorption for target 2°Ab.

3.4. Sensitivity measurement

The sensitivity of the PPa/1°Ab-coated TiO_2-NW FET device was examined by adding various concentrations of target 2°Ab. After affinity adsorption, the device was connected to the measurement system, and the electrical responses from the analyte were recorded and analyzed. Fig. 6 shows that PPa/1°Ab-functionalized TiO_2-NW biosensors have high specificity and selectivity with good sensitivity towards target 2°Ab, due to the specific antibody–antigen reaction. The device was first exposed to the mixture solution containing 119 pg/mL of 2°Ab. After the un-adsorbed proteins in the solution were removed, a significant change in the I_D curve was measured for the surface-dried TiO_2-NW FET device. The device was further tested in a solution containing 2°Ab, which was increased from low to high concentration. Stepwise-increasing affinity adsorption and measurement (I_D–V_{DS}) procedures were performed at each concentration, as shown in Fig. 6a. The slope of the measured I_D decreased when the concentration of the target 2°Ab was increased. Calculations of I_D changes at various protein concentrations at 5 V of applied voltage were undertaken to determine the performance and sensitivity of the NW FET biosensor (Fig. 6b). Under the study concentrations ranging from 119 pg/mL to 5.95 ng/mL, the limits of detection (LOD) for 5 V of the applied V_{DS} were −3.96 A/(ng/mL) and R-square = 0.903. Such operating conditions should be important for the sensitivity and LOD of our TiO_2-NW-based FET biosensors.

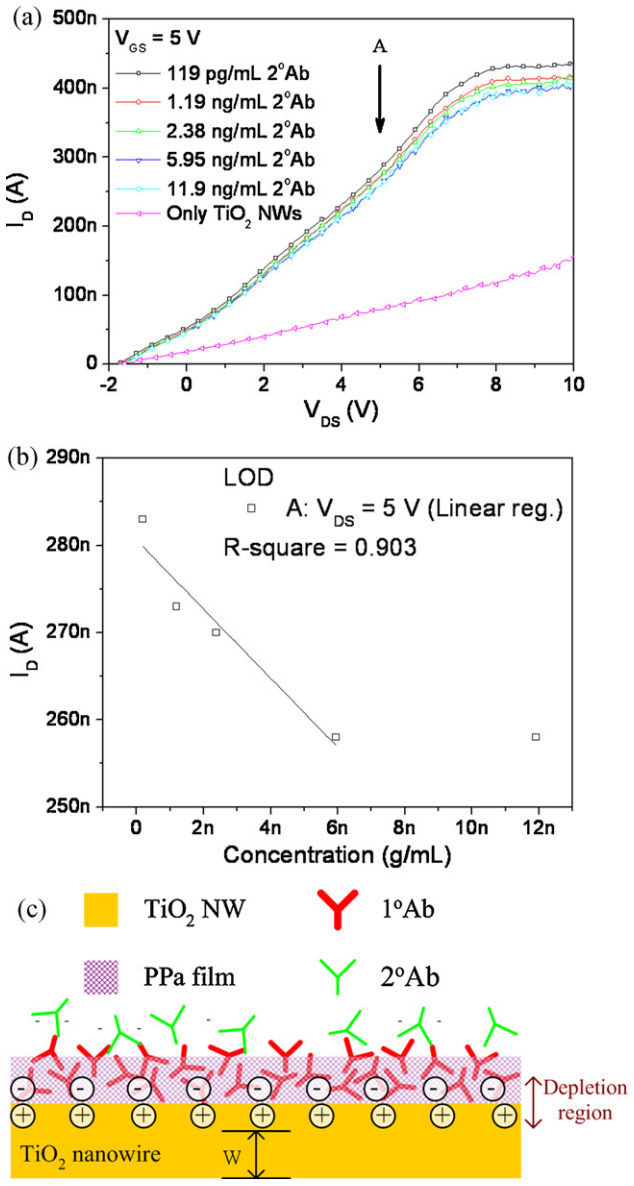

Fig. 6. I_D–V_{DS} curve showing the response of the TiO_2-NW-based immunosensor after immunoreactions with various concentrations of 2°Ab. (a) The I_D–V_{DS} curve decreased when the concentration of 2°Ab was changed from low to high. (b) The immunoresponse of TiO_2-NW-based immunosensor exhibited a linear region (V_{DS} = 5 V) at 2°Ab concentrations lower than 5.95 ng/mL. (c) Schematic diagram of the NWs/PPa/1°Ab surface showing negative charges, even when the adsorbed 2°Ab concentration increased. A positive space charge might form near the NW side, increasing the depletion region and the channel resistance.

Once antigens or antibodies (usually negatively charged) are affinity adsorbed on a bio-functionalized NW surface, a few charges or carriers can follow the conducting path through the PPa layer. I_D decreased when the sensor surface had more immunoreactions, and, according to Curreli and Zhang, an electrical field may be created on the NW surface or inside and outside the semiconductor conducting channel (Curreli et al., 2008). As shown in Fig. 6c, the saturated conducting path may have a positive effect on the conducting channel of TiO_2 NWs. The negatively charged 2°Ab, acting as electron carriers, becomes the main carrier of the n-type TiO_2-NW FET. As the electron carriers might deplete after the affinity bounding of 2°Ab, the density of all mobile carriers becomes zero in this area (depletion region) with a decreasing tendency of I_D. These findings are consistent with those reported in Lieber and other studies (Patolsky et al., 2006b; Curreli et al., 2008; Li et al., 2005).

Several implications for 1-D nanomaterial FETs biosensor can be drawn from this study. The TiO_2-NW-based FET immunosensor reported in this paper has demonstrated that the encapsulation of biomolecules by PPa can be practically implemented and provide adequate results, as a significant improvement in biomolecule immobilization at specific regions was obtained in this work. An important area for future research will be in refinement of approaches to NW deposition/alignment on a substrate. In addition, more tests should be performed, including those that focus on the reliability and repeatability of similar designs. Another interesting avenue of investigation might be the potential of TiO_2 materials for use in photo-electric-based biosensors.

4. Conclusions

A TiO_2-NW-based FET immunosensor with the ECP of low-conductivity PPa/1°Ab-coated film on the NW surface was demonstrated. EDS analysis shows that the carbon element on the PPa/1°Ab-coated TiO_2 NWs had a significantly higher weight ratio than that of the control group. Electrical analysis indicates that the current change (I_D) on the bio-functionalized immunosensor was larger than that of the PPa-coated group. The FET immunosensor developed in this work can be used for the detection of rabbit IgG in a linear range of 119 pg/mL–5.95 ng/mL, with *R*-square values of 0.903 for the linear region (V_{DS} = 5 V). A low-conductivity polymer was used as the encapsulation matrix for the ECP of biomolecules.

Acknowledgements

The authors would like to thank Prof. Jih-Jen Wu and Mr. Wei-Ting Wu in the Department of Chemical Engineering, NCKU, for material preparation and their helpful comments, and Prof. Hong-Ping Lin at the Department of Chemistry, NCKU, for TEM assistance. We also like to thank Prof. Jyh-Ling Lin and Dr. Ta-Chuan Liao at the Department of Electronic Engineering, HFU and NCTU for technical support.

The work was supported with funding from the Ministry of (459) Education, Taiwan under the NCKU Project of Promoting Academic (460) Excellence & Developing World Class Research Centers (R017), as well as the Multidisciplinary Center of Excellence for Clinical Trial and Research (DOH99-TD-B-111-102), Department of Health, Executive Yuan, Taiwan.

References

Bao, S.J., Li, C.M., Zang, J.F., Cui, X.Q., Qiao, Y., Guo, J., 2008. Adv. Funct. Mater. 18 (4), 591–599.
Byon, H.R., Kim, S., Choi, H.C., 2008. Nano 3 (6), 415–431.
Chen, W., Lei, Y., Li, C.M., 2010. Electroanalysis 22 (10), 1078–1083.
Cosnier, S., Senillou, A., Gratzel, M., Comte, P., Vlachopoulos, N., Renault, N.J., Martelet, C., 1999. J. Electroanal. Chem. 469 (2), 176–181.
Cui, Y., Wei, Q.Q., Park, H.K., Lieber, C.M., 2001a. Science 293 (5533), 1289–1292.
Cui, X.Y., Lee, V.A., Raphael, Y., Wiler, J.A., Hetke, J.F., Anderson, D.J., Martin, D.C., 2001b. J. Biomed. Mater. Res. A 56 (2), 261–272.
Curreli, M., Zhang, R., Ishikawa, F.N., Chang, H.K., Cote, R.J., Zhou, C., Thompson, M.E., 2008. IEEE Trans. Nanotechnol. 7 (6), 651–667.
Dong, H., Li, C.M., Chen, W., Zhou, Q., Zeng, Z.X., Luong, J.H.T., 2006. Anal. Chem. 78 (21), 7424–7431.
Dong, H., Li, C.M., Zhang, Y.F., Cao, X.D., Gan, Y., 2007. Lab Chip 7 (12), 1752–1758.
Dong, H., Cao, X.D., Li, C.M., Hu, W.H., 2008. Biosens. Bioelectron. 23 (7), 1055–1062.
Gerard, M., Chaubey, A., Malhotra, B.D., 2002. Biosens. Bioelectron. 17 (5), 345–359.
He, B., Morrow, T.J., Keating, C.D., 2008. Curr. Opin. Chem. Biol. 12 (5), 522–528.
Hu, W.H., Li, C.M., Cui, X.Q., Dong, H., Zhou, Q., 2007. Langmuir 23 (5), 2761–2767.
Hu, W.H., Li, C.M., Dong, H., 2008. Anal. Chim. Acta 630 (1), 67–74.
Hu, W.H., Lu, Z.S., Liu, Y.S., Li, C.M., 2010. Langmuir 26 (11), 8386–8391.
Jin, S., Whang, D.M., McAlpine, M.C., Friedman, R.S., Wu, Y., Lieber, C.M., 2004. Nano Lett. 4 (5), 915–919.
Katz, E., Willner, I., 2004. ChemPhysChem 5 (8), 1085–1104.

Kum, M.C., Joshi, K.A., Chen, W., Myung, N.V., Mulchandani, A., 2007. Talanta 74 (3), 370–375.
Kwon, N.H., Rahman, M.A., Won, M.S., Shim, Y.B., 2006. Anal. Chem. 78 (1), 52–60.
Lange, U., Roznyatouskaya, N.V., Mirsky, V.M., 2008. Anal. Chim. Acta 614 (1), 1–26.
Li, C., Curreli, M., Lin, H., Lei, B., Ishikawa, F.N., Datar, R., Cote, R.J., Thompson, M.E., Zhou, C.W., 2005. J. Am. Chem. Soc. 127 (36), 12484–12485.
Li, R., Gan, Y., Song, Q.L., Zhu, Z.H., Shi, J.S., Yang, H.B., Wang, W., Chen, P., Li, C.M., 2010. Nanoscale 2 (8), 1474–1479.
Lu, Q., Li, C.M., 2008. Biosens. Bioelectron. 24 (4), 767–772.
Papp, S., Korosi, L., Meynen, V., Cool, P., Vansant, E.F., Dekany, I., 2005. J. Solid State Chem. 178 (5), 1614–1619.
Patolsky, F., Zheng, G.F., Lieber, C.M., 2006a. Anal. Chem. 78 (13), 4260–4269.
Patolsky, F., Zheng, G.F., Lieber, C.M., 2006b. Nat. Protoc. 1 (4), 1711–1724.
Ramanathan, K., Bangar, M.A., Yin, M.H., Chen, W., Mulchandani, A., Myung, N.V., 2007. Electroanalysis 19 (7–8), 793–797.
Star, A., Gabriel, J.C.P., Bradley, K., Gruner, G., 2003. Nano Lett. 3 (4), 459–463.
Storri, S., Santoni, T., Minunni, M., Mascini, M., 1998. Biosens. Bioelectron. 13 (3–4), 347–357.
Varghese, O.K., Gong, D.W., Paulose, M., Ong, K.G., Grimes, C.A., 2003. Sens. Actuators B 93 (1–3), 338–344.
Wang, R.H., Ruan, C.M., Kanayeva, D., Lassiter, K., Li, Y.B., 2008. Nano Lett. 8 (9), 2625–2631.
Wilson, M.S., Nie, W.Y., 2006. Anal. Chem. 78 (8), 2507–2513.
Zheng, G.F., Patolsky, F., Cui, Y., Wang, W.U., Lieber, C.M., 2005. Nat. Biotechnol. 23 (10), 1294–1301.